ASME Letters in Dynamic Systems and Control
Online journal at:
https://asmedigitalcollection.asme.org/lettersdynsys

Reactive Collision Avoidance Control for Nonholonomic Vehicles and Obstacles of Arbitrary Shape

Erick J. Rodríguez-Seda
Department of Weapons, Robotics, and Control Engineering,
United States Naval Academy,
Annapolis, MD 21402
e-mail: rodrigue@usna.edu

Potential field-based collision avoidance algorithms for mobile robots frequently assume vehicles and obstacles to have circular or spherical shapes. This assumption not only simplifies the analysis but also limits the mobility of agents in confined spaces, particularly for vehicles with elongated or irregular shapes. To increase mobility, this letter presents a decentralized collision avoidance framework for nonholonomic systems of unicycle type that considers the non-circular shape and relative orientation of vehicles and obstacles. The framework builds on the concepts of potential field and avoidance functions. However, it proposes using a non-constant minimum safe distance radius that changes based on the shape, relative position, and relative orientation of agents. The control framework is proven to guarantee collision avoidance at all times and is shown, via simulation, to increase the ability of agents to navigate through narrow spaces safely.
[DOI: 10.1115/1.4065644]

Keywords: multi-vehicle systems, obstacle avoidance, potential field functions, decentralized control, cooperative control

1 Introduction

A critical task of mobile robots is the ability to follow a desired trajectory or path while avoiding collisions with other vehicles and obstacles. Methods for collision avoidance include the use of velocity obstacle [1] and its variants [2,3], the concept of collision cones [4,5], the use of potential field functions [6–9], and the implementation of barrier functions [10,11], to name a few (see Refs. [12–14] for comprehensive reviews). A common assumption among most of these methods is the generalization of agents (namely, vehicles and obstacles) as having circular or spherical shapes. Although this assumption simplifies the analysis and implementation, it is also overly conservative, particularly for agents with elongated shapes. For instance, consider the two vehicles in Fig. 1, which have nearly rectangular shapes. The circular body assumption will require both vehicles to keep a distance from each other equal to or larger than the summation of their circumradii, $r_{ij}^{\max} = h_i + h_j$, regardless of their relative orientation. That is, the circular shape assumes the worst-case scenario and makes the vehicles occupy a larger space than necessary, which can impede the motion of agents in cluttered spaces and narrow corridors [15]. Therefore, for confined environments, it is more suitable to design avoidance control strategies that take the vehicle's and the obstacle's shape into consideration.

Examples of control algorithms that explicitly consider the non-circular shape of agents include methods based on reachability concepts. For instance, Ref. [4] introduces a collision cone approach for dynamic obstacles of arbitrary shape, which is later extended to obstacles of deformable shape [15] and to nonholonomic vehicles [5]. In Ref. [16], a distance-projection method is formulated using reachable sets that take into account the shape and kinematics of vehicles and obstacles. A common drawback of the aforementioned methods is that, with a large number of dynamic obstacles, they either cannot guarantee collision avoidance or the problem can quickly become intractable.

Collision avoidance with objects of non-circular shape has also been approached using potential field functions, which have the typical advantage of generating methods that can be rigorously proven to be safe for an arbitrarily large number of obstacles. However, most of these approaches rely on computing the closest distance to the obstacle [6] or a set of points in its boundary [17], which can generate non-smooth control inputs, be computationally expensive, or not suitable for non-convex obstacles. Others have approximated the shape of elongated agents using ellipsoids [7,18,19], which can still introduce conservatism for objects of irregular shape. Another common approach is representing the obstacles as an assemblage of n-dimensional small spheres [20] and ellipsoids [18]. However, these methods would require a collision avoidance action for each individual surface.

Recently, gradient-based optimization methods have been proposed using signed distance functions [21,22] and control barrier functions [10,11,23]. For instance, the work in Ref. [21] introduces an optimization scheme to determine collision-free trajectories by approximating the gradient of signed distance functions to obstacles

Manuscript received February 9, 2024; final manuscript received May 28, 2024; published online June 24, 2024. Assoc. Editor: Santhakumar Mohan.

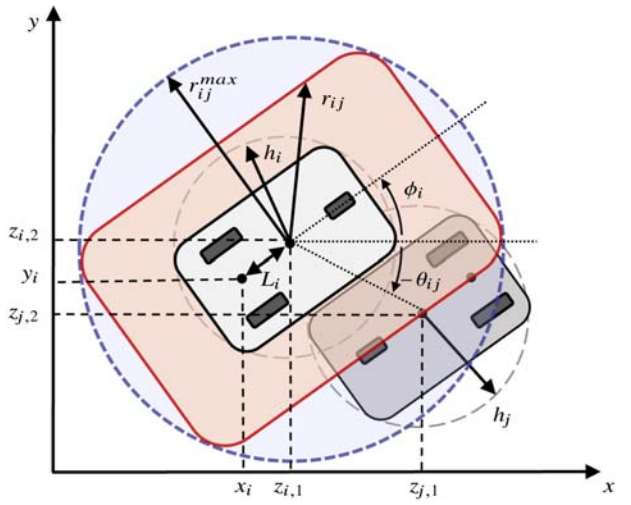

Fig. 1 Safe minimum distance for two vehicles of rectangular shape with circumradii h_i and h_j. Traditional approaches assume circular shapes and enforce a constant minimum distance equal to or greater than $r_{ij}^{max} = h_i + h_j$, which is the minimum safe distance when the agents are parallel to each other and diagonally opposed. This results in an excessive separation at any other configuration.

of primitive shapes. Similarly, Ref. [11] introduces the use of control barrier functions to guarantee the safety of vehicles with limited actuation. Yet, many of these approaches do not yield controllers in closed form or may yield discontinuous control inputs due to the approximations.

In this letter, we present a decentralized, reactive potential field-based collision avoidance method for an arbitrarily large group of nonholonomic vehicles of unicycle type and arbitrary shape. We use the concept of avoidance functions presented in Ref. [7] and extend it to vehicles and obstacles of arbitrary shape by introducing a non-constant minimum safe distance. The minimum safe distance (or avoidance radius) is a function of the relative orientation between the obstacle and the vehicle, as well as their shapes. Unlike previous potential field-based frameworks, ours only requires a single function between pairs of agents and generates analytical, smooth control inputs. To prevent deadlocks, a common drawback of potential field methods [17], we include an almost everywhere continuous and smooth control perturbation aimed to break symmetries in the potential field. The overall control strategy is rigorously proven to avoid collision among cooperative vehicles and static obstacles at all times. We validate the control approach via a numerical example with vehicles and obstacles of rectangular shape. To the best of our knowledge, this is the first time that a time-varying avoidance radius or minimum safe distance is assumed within the avoidance functions framework [7].

2 Problem Formulation

2.1 Multi-Vehicle Dynamics. We consider the task of safely coordinating the motion of N vehicles with nonholonomic dynamic equations given by

$$\begin{aligned} \dot{x}_i(t) &= v_i(t)\cos\phi_i(t), \quad m_i\dot{v}_i(t) = f_i(t), \\ \dot{y}_i(t) &= v_i(t)\sin\phi_i(t), \quad J_i\dot{\omega}_i(t) = \tau_i(t), \\ \dot{\phi}_i(t) &= \omega_i(t) \end{aligned} \tag{1}$$

where $x_i(t)$ and $y_i(t)$ are the position coordinates, $\phi_i(t)$ is the orientation, $v_i(t)$ and $\omega_i(t)$ are the linear and angular velocities, m_i is the mass, J_i is the inertia, and $f_i(t)$ and $\tau_i(t)$ are the control force and torque inputs for the ith robot (see Fig. 1). In what follows, we will omit the time argument of signals unless deemed necessary.

It is well known that the position and orientation of (1) cannot be simultaneously stabilized at a desired value using a continuous static state feedback control law [24]. Therefore, we will opt to control a reference point in front of (x_i, y_i), see Fig. 1, given by

$$z_{i,1} = x_i + L_i\cos\phi_i, \quad z_{i,2} = y_i + L_i\sin\phi_i \tag{2}$$

where $L_i > 0$ is a constant parameter [25] and $\mathbf{z}_i = [z_{i,1}, z_{i,2}]^T$ is the Cartesian position of the reference point. If we take the first and second derivatives of (2) and apply the following control inputs to (1)

$$\begin{bmatrix} f_i \\ \tau_i \end{bmatrix} = \begin{bmatrix} \dfrac{\cos\phi_i}{m_i} & \dfrac{\sin\phi_i}{m_i} \\ \dfrac{-\sin\phi_i}{J_iL_i} & \dfrac{\cos\phi_i}{J_iL_i} \end{bmatrix} \begin{bmatrix} u_{i,1} + v_i\omega_i\sin\phi_i + L_i\omega_i^2\cos\phi_i \\ u_{i,2} - v_i\omega_i\cos\phi_i + L_i\omega_i^2\sin\phi_i \end{bmatrix} \tag{3}$$

one can show that (1) reduces to

$$\ddot{\mathbf{z}}_i = \mathbf{u}_i \tag{4a}$$

$$\dot{\phi}_i = \begin{bmatrix} -\dfrac{\sin\phi_i}{L_i} & \dfrac{\cos\phi_i}{L_i} \end{bmatrix} \dot{\mathbf{z}}_i \tag{4b}$$

where $\mathbf{u}_i = [u_{i,1}, u_{i,2}]^T$ is the control input for the linearized system. While the internal dynamics (4*b*) can only be shown to be Lagrange stable [12], the linear dynamics of the reference point (4*a*) are controllable. That is, for any desired trajectory $\mathbf{z}_i^d \in \mathbb{R}^2$, one can design a state feedback control law $\mathbf{u}_i$ such that $\mathbf{z}_i \to \mathbf{z}_i^d$ as $t \to \infty$.

2.2 Minimum Safe Distance. Herein, we would like the vehicles to maintain a safe distance from each other as well as obstacles. Accordingly, we define the minimum safe distance between the ith vehicle and jth agent as

$$r_{ij} := r_{ij}(\mathbf{z}_i, \mathbf{z}_j, \phi_i, \phi_j) = r_{ji}(\mathbf{z}_j, \mathbf{z}_i, \phi_j, \phi_i) \tag{5}$$

where r_{ij} takes into account the shape, relative position, and orientation of agents, as illustrated in Fig. 1. We say that a collision between agents takes place if $\|\mathbf{z}_i - \mathbf{z}_j\| \le r_{ij}$ for some time t. It is assumed that r_{ij} is time continuous differentiable and symmetric (i.e., $r_{ij} = r_{ji}$), yet it may differ among different pairs of agents (i.e., $r_{ij} \equiv r_{ik}$ for $j \neq k$). An example of a smooth analytical expression for vehicles and obstacles with rectangular shapes is given in Sec. 4.

2.3 Control Objective. The ith vehicle's ultimate control objective is to follow a desired trajectory, given as $\mathbf{z}_i^d \in \mathbb{R}^2$, while maintaining a safe distance r_{ij} from other vehicles and obstacles at all times. To this end, we assume that each vehicle can detect, either via communication or onboard sensors, the relative position and orientation of other agents within a bounded detection radius R, where $R > \sup_{i,j\neq i}\{r_{ij}\} = r_{ij}^{\max}$. Then, we can formulate the control objective as follows. Design a control strategy $\mathbf{u}_i$ such that $\mathbf{z}_i \to \mathbf{z}_i^d$ as $t \to \infty$ and $\|\mathbf{z}_i - \mathbf{z}_j\| > r_{ij}\ \forall\ i, j \neq i,\ t \ge 0$.

3 Trajectory Tracking With Collision Avoidance Control

3.1 Avoidance Functions. For the purpose of avoidance control, we use the concept of avoidance functions. Similar to Ref. [7], we define an avoidance function between the ith vehicle and jth agent as

$$V_{ij} := V_{ij}(\mathbf{z}_i, \mathbf{z}_j, r_{ij}) = \left(\min\left\{0, \frac{\|\mathbf{z}_i - \mathbf{z}_j\|^2 - R_{ij}^2}{\|\mathbf{z}_i - \mathbf{z}_j\|^2 - r_{ij}^2}\right\}\right)^2 \tag{6}$$

where the reaction distance (i.e., the distance at which the vehicle starts avoiding the obstacle) is defined as $R_{ij} = r_{ij} + \Delta_R$ for some positive constant $\Delta_R \in (0, R - r_{ij}^{\max})$. One can show that V_{ij} is almost everywhere continuously differentiable, that

$$\frac{\partial V_{ij}}{\partial \mathbf{z}_i} = \frac{\partial V_{ji}}{\partial \mathbf{z}_i}, \quad \frac{\partial V_{ij}}{\partial \mathbf{z}_i} = -\frac{\partial V_{ij}}{\partial \mathbf{z}_j}, \quad \frac{\partial V_{ij}}{\partial r_{ij}} = \frac{\partial V_{ji}}{\partial r_{ij}} \tag{7}$$

and that

$$\frac{\partial V_{ij}^T}{\partial \mathbf{z}_i} = \frac{4(R_{ij} - r_{ij})(\|\mathbf{z}_i - \mathbf{z}_j\|^2 - R_{ij}^2)(\mathbf{z}_i - \mathbf{z}_j)}{(\|\mathbf{z}_i - \mathbf{z}_j\|^2 - r_{ij}^2)^3} \tag{8}$$

$$\frac{\partial V_{ij}}{\partial r_{ij}} = \frac{4\Delta_R(R_{ij}^2 - \|\mathbf{z}_i - \mathbf{z}_j\|^2)(r_{ij}R_{ij} + \|\mathbf{z}_i - \mathbf{z}_j\|^2)}{(\|\mathbf{z}_i - \mathbf{z}_j\|^2 - r_{ij}^2)^3} \tag{9}$$

if $r_{ij} < \|\mathbf{z}_i - \mathbf{z}_j\| \leq R_{ij}$, undefined if $\|\mathbf{z}_i - \mathbf{z}_j\| = r_{ij}$, and zero otherwise. In addition, due to the symmetry of the avoidance functions, we have that

$$\begin{aligned}\sum_{i=1}^{N}\sum_{j\in N_i}&\left(\frac{\partial V_{ij}}{\partial \mathbf{z}_i}\dot{\mathbf{z}}_i + \frac{\partial V_{ij}}{\partial r_{ij}}\frac{\partial r_{ij}}{\partial \mathbf{z}_i}\dot{\mathbf{z}}_i + \frac{\partial V_{ij}}{\partial r_{ij}}\frac{\partial r_{ij}}{\partial \phi_i}\dot{\phi}_i\right)\\ &= \frac{1}{2}\sum_{i=1}^{N}\sum_{j\in N_i}\left(\frac{\partial V_{ij}}{\partial \mathbf{z}_i}\dot{\mathbf{z}}_i + \frac{\partial V_{ij}}{\partial r_{ij}}\frac{\partial r_{ij}}{\partial \mathbf{z}_i}\dot{\mathbf{z}}_i + \frac{\partial V_{ij}}{\partial r_{ij}}\frac{\partial r_{ij}}{\partial \phi_i}\dot{\phi}_i\right.\\ &\left. + \frac{\partial V_{ij}}{\partial \mathbf{z}_j}\dot{\mathbf{z}}_j + \frac{\partial V_{ij}}{\partial r_{ij}}\frac{\partial r_{ij}}{\partial \mathbf{z}_j}\dot{\mathbf{z}}_j + \frac{\partial V_{ij}}{\partial r_{ij}}\frac{\partial r_{ij}}{\partial \phi_j}\dot{\phi}_j\right) = \frac{1}{2}\sum_{i=1}^{N}\sum_{j\in N_i}\dot{V}_{ij}\end{aligned} \tag{10}$$

Note that different to other definitions of avoidance functions [7,8], the ones defined here use a non-constant safe distance r_{ij} and a non-constant reaction distance R_{ij}. It is worth mentioning that the work in Refs. [26,27] uses a time-varying velocity-based reaction distance, R_{ij}.

3.2 Control Law. To achieve the tracking and collision avoidance objective, we propose the control input to be given by

$$\mathbf{u}_i = \ddot{\mathbf{z}}_i^d + K_v(\dot{\mathbf{z}}_i^d - \dot{\mathbf{z}}_i) + K_p(\mathbf{z}_i^d - \mathbf{z}_i) + \mathbf{u}_i^a + \mathbf{u}_i^p \tag{11a}$$

$$\mathbf{u}_i^a = -\sum_{j\in N_i}\left(\frac{\partial V_{ij}^T}{\partial \mathbf{z}_i} + \frac{\partial V_{ij}}{\partial r_{ij}}\frac{\partial r_{ij}}{\partial \mathbf{z}_i}^T + \frac{1}{L_i}\frac{\partial V_{ij}}{\partial r_{ij}}\frac{\partial r_{ij}}{\partial \phi_i}\begin{bmatrix}-\sin\phi_i\\ \cos\phi_i\end{bmatrix}\right) \tag{11b}$$

$$\mathbf{u}_i^p = \frac{\lambda_1 \mathcal{R}((\pi/2) - \vartheta_i)\mathbf{u}_a \cos(\sigma_i t)}{\|\mathbf{u}_i^a\| + \|\dot{\mathbf{z}}_i\|^{\lambda_2} + \lambda_3} \tag{11c}$$

where K_v, K_p, λ_*, and σ_i are all positive constants, N_i is the set of neighbors for the ith agent, ϑ_i is the angle between $\mathbf{u}_i^a$ and $\dot{\mathbf{z}}_i^d - \dot{\mathbf{z}}_i$, and $\mathcal{R}(\cdot)$ is the 2×2 rotational matrix. The first three terms in (11a) comprise the trajectory tracking control law, with K_v and K_p regulating the convergence rate (to be shown next). The term $\mathbf{u}_i^a$ is the cooperative collision avoidance strategy and $\mathbf{u}_i^p$ is an optional control perturbation aimed to reduce the occurrence of unwanted local minima (i.e., deadlocks). Note that $\mathbf{u}_i^a$ is only active when another vehicle or obstacle is within the reaction distance R_{ij}. In addition, note that $\mathbf{u}_i^p$ is upper bounded by λ_1, almost everywhere continuous (except at $\mathbf{u}_i^a = \mathbf{0}$ or $\dot{\mathbf{z}}_i^d - \dot{\mathbf{z}}_i = \mathbf{0}$), null if there is no collision threat, and always perpendicular to $\dot{\mathbf{z}}_i^d - \dot{\mathbf{z}}_i$. To prove the latter, it is sufficient to show that $(\dot{\mathbf{z}}_i^d - \dot{\mathbf{z}}_i)^T\mathcal{R}(\pi/2) - \vartheta_i)\mathbf{u}_i^a = 0$. Therefore, let $\dot{\mathbf{z}}_i^d - \dot{\mathbf{z}}_i = [a, b]^T$ and $\mathbf{u}_i^a = [c, d]^T$. Then,

$$\begin{aligned}[a\ \ b]\mathcal{R}\left(\frac{\pi}{2} - \vartheta_i\right)\begin{bmatrix}c\\ d\end{bmatrix} &= [a\ \ b]\begin{bmatrix}\sin\vartheta_i & -\cos\vartheta_i\\ \cos\vartheta_i & \sin\vartheta_i\end{bmatrix}\begin{bmatrix}c\\ d\end{bmatrix}\\ &= \sin\vartheta_i(ac + bd) - \cos\vartheta_i(ad - bc)\\ &= \frac{(ad - bc)(ac + bd)}{\|[a\ \ b]^T\|\|[c\ \ d]^T\|} - \frac{(ac + bd)(ad - bc)}{\|[a\ \ b]^T\|\|[c\ \ d]^T\|} = 0\end{aligned} \tag{12}$$

where we used the dot and cross product formulas for finding ϑ_i. Finally, the cosine function in $\mathbf{u}_i^p$ aims to keep the perturbation persistently exciting, changing the direction of the perturbation vector at a frequency given by σ_i.

Similar to Ref. [8], we now make the following assumption about the desired trajectory.

ASSUMPTION 1. *The desired trajectory satisfies the following constraint:* $\dot{\mathbf{z}}_i^{dT}\mathbf{u}_i^a \leq K_v\|\dot{\mathbf{z}}_i^d - \dot{\mathbf{z}}_i\|^2$ *for all* $t \geq 0$.

Note that Assumption 1 is trivially satisfied when the desired trajectory is constant $\dot{\mathbf{z}}_i^d = \ddot{\mathbf{z}}_i^d = \mathbf{0}$. In the case of non-constant trajectory, we can assume that the ith robot can momentarily freeze the desired trajectory while trying to resolve a collision conflict, similar to Ref. [8], or when $\dot{\mathbf{z}}_i^{dT}\mathbf{u}_i^a > K_v\|\dot{\mathbf{z}}_i^d - \dot{\mathbf{z}}_i\|^2$.

THEOREM 1 (Collision avoidance). *Consider the system in* (1) *with control law* (3) *and* (11). *Suppose Assumption 1 holds. If* $\|\mathbf{z}_i(0) - \mathbf{z}_j(0)\| > r_{ij}\ \forall\ i, j \neq i$, *then* $\|\mathbf{z}_i(t) - \mathbf{z}_j(t)\| > r_{ij}\ \forall t \geq 0$.

Proof. Consider the following Lyapunov function:

$$W_c = \frac{1}{2}\sum_{i=1}^{N}\left(K_p\|\mathbf{z}_i^d - \mathbf{z}_i\|^2 + \|\dot{\mathbf{z}}_i^d - \dot{\mathbf{z}}_i\|^2 + \sum_{j\in N_i}V_{ij}\right) \tag{13}$$

Taking its time derivative yields

$$\begin{aligned}\dot{W}_c = &\sum_{i=1}^{N}\left(K_p(\mathbf{z}_i^d - \mathbf{z}_i)^T(\dot{\mathbf{z}}_i^d - \dot{\mathbf{z}}_i) + (\dot{\mathbf{z}}_i^d - \dot{\mathbf{z}}_i)^T(\ddot{\mathbf{z}}_i^d - \mathbf{u}_i)\right)\\ &+ \frac{1}{2}\sum_{i=1}^{N}\sum_{j\in N_i}\left(\frac{\partial V_{ij}}{\partial \mathbf{z}_i}\dot{\mathbf{z}}_i + \frac{\partial V_{ij}}{\partial \mathbf{z}_i}\dot{\mathbf{z}}_j + \frac{\partial V_{ij}}{\partial r_{ij}}\frac{\partial r_{ij}}{\partial \mathbf{z}_i}\dot{\mathbf{z}}_i\right.\\ &\left. + \frac{\partial V_{ij}}{\partial r_{ij}}\frac{\partial r_{ij}}{\partial \mathbf{z}_j}\dot{\mathbf{z}}_j + \frac{\partial V_{ij}}{\partial r_{ij}}\frac{\partial r_{ij}}{\partial \boldsymbol{\phi}_i}\dot{\phi}_i + \frac{\partial V_{ij}}{\partial r_{ij}}\frac{\partial r_{ij}}{\partial \boldsymbol{\phi}_j}\dot{\phi}_j\right)\end{aligned} \tag{14}$$

and substituting for (11) and (10), one obtains that

$$\begin{aligned}\dot{W}_c = &\sum_{i=1}^{N}\left(-K_v\|\dot{\mathbf{z}}_i^d - \dot{\mathbf{z}}_i\|^2 - \dot{\mathbf{z}}_i^{dT}\mathbf{u}_i^a - \sum_{j\in N_i}\frac{\partial V_{ij}}{\partial \mathbf{z}_i}\dot{\mathbf{z}}_i\right.\\ &\left. - \sum_{j\in N_i}\frac{\partial V_{ij}}{\partial r_{ij}}\frac{\partial r_{ij}}{\partial \mathbf{z}_i}\dot{\mathbf{z}}_i - \sum_{j\in N_i}\frac{\partial V_{ij}}{\partial r_{ij}}\frac{\partial r_{ij}}{\partial \phi_i}\underbrace{\begin{bmatrix}-\sin\phi_i\\ \cos\phi_i\end{bmatrix}^T\cdot\frac{\dot{\mathbf{z}}_i}{L_i}}_{=\dot{\phi}_i}\right)\\ &+ \sum_{i=1}^{N}\sum_{j\in N_i}\left(\frac{\partial V_{ij}}{\partial \mathbf{z}_i}\dot{\mathbf{z}}_i + \frac{\partial V_{ij}}{\partial r_{ij}}\frac{\partial r_{ij}}{\partial \mathbf{z}_i}\dot{\mathbf{z}}_i + \frac{\partial V_{ij}}{\partial r_{ij}}\frac{\partial r_{ij}}{\partial \phi_i}\dot{\phi}_i\right)\\ &= \sum_{i=1}^{N}\left(-K_v\|\dot{\mathbf{z}}_i^d - \dot{\mathbf{z}}_i\|^2 - \dot{\mathbf{z}}_i^{dT}\mathbf{u}_i^a\right) \leq 0\end{aligned} \tag{15}$$

where we used Assumption 1. Since $\dot{W}_c \leq 0$, we have that W_c is bounded for all $t \geq 0$, that is, $W_c(t) \leq W_c(0) \leq \infty$. Now, suppose that for some pair $i, j \neq i$ we have that $\|\mathbf{z}_i(t) - \mathbf{z}_j(t)\| \to r_{ij}$. The latter would imply that $W_c \to \infty$, which is a contradiction. Therefore, we have that $\|\mathbf{z}_i(t) - \mathbf{z}_j(t)\| > r_{ij}\ \forall\ i, j \neq i$ and $t \geq 0$. ∎

THEOREM 2 (Trajectory tracking). *Assume that* $\exists\ t_0 \geq 0$ *such that* $\|\mathbf{z}_i(t) - \mathbf{z}_j(t)\| \geq R_{ij}\ \forall\ j \neq i$ *and* $\forall\ t \geq t_0$. *Then,* $(\mathbf{z}_i(t), \dot{\mathbf{z}}_i(t))$ *converges to* $(\mathbf{z}_i^d(t), \dot{\mathbf{z}}_i^d(t))$ *exponentially as* $t \to \infty$.

Proof. Let $\tilde{\mathbf{z}}_i = \mathbf{z}_i^d - \mathbf{z}_i$ and consider the following Lyapunov function:

$$W_T = K_p\|\tilde{\mathbf{z}}_i\|^2 + \frac{1}{2}\left\|\dot{\tilde{\mathbf{z}}}_i\right\|^2 + \frac{1}{2}\left\|\dot{\tilde{\mathbf{z}}}_i + K_v\tilde{\mathbf{z}}_i\right\|^2 \tag{16}$$

which is lower and upper bounded by

$$\alpha_1\left\|[\tilde{\mathbf{z}}_i^T, \dot{\tilde{\mathbf{z}}}_i^T]\right\|^2 \le W_T \le \alpha_2\left\|[\tilde{\mathbf{z}}_i^T, \dot{\tilde{\mathbf{z}}}_i^T]\right\|^2 \tag{17}$$

for $\alpha_1 = \min\{1/2, K_p\} < \alpha_2 = \max\{3/2, K_p + K_v^2\}$. Taking its time derivative yields

$$\dot{W}_T = 2K_p\tilde{\mathbf{z}}_i^T\dot{\tilde{\mathbf{z}}}_i + \dot{\tilde{\mathbf{z}}}_i^T\ddot{\tilde{\mathbf{z}}}_i + (\dot{\tilde{\mathbf{z}}}_i + K_v\tilde{\mathbf{z}}_i)^T(\ddot{\tilde{\mathbf{z}}}_i + K_v\dot{\tilde{\mathbf{z}}}_i) \tag{18}$$

Now, the assumption that $\exists\ t_0 \ge 0$ such that $\|\mathbf{z}_i(t) - \mathbf{z}_j(t)\| \ge R_{ij}\ \forall\ j \ne i$ and $\forall\ t \ge t_0$ implies that $\mathbf{u}_i^a = \mathbf{u}_i^p = \mathbf{0}\ \forall\ t \ge t_0$. Then, returning to (18) yields that

$$\dot{W}_T = -K_pK_v\|\tilde{\mathbf{z}}_i\|^2 - K_v\left\|\dot{\tilde{\mathbf{z}}}_i\right\|^2 \le -\alpha_3\left\|[\tilde{\mathbf{z}}_i^T, \dot{\tilde{\mathbf{z}}}_i^T]\right\|^2 \tag{19}$$

where $\alpha_3 = \min\{K_v, K_pK_v\}$. Applying [28, Theorem 4.10], one can conclude that the pair $\tilde{\mathbf{z}}_i(t)$ and $\dot{\tilde{\mathbf{z}}}_i(t)$ converge to zero exponentially, for all $t \ge t_0$, i.e.,

$$\left\|\begin{bmatrix}\tilde{\mathbf{z}}_i(t)\\ \dot{\tilde{\mathbf{z}}}_i(t)\end{bmatrix}\right\| \le \sqrt{\frac{\alpha_2}{\alpha_1}}\cdot\left\|\begin{bmatrix}\tilde{\mathbf{z}}_i(t_0)\\ \dot{\tilde{\mathbf{z}}}_i(t_0)\end{bmatrix}\right\| e^{-(\alpha_3(t-t_0)/2\alpha_2)}, \quad t \ge t_0 \tag{20}$$

■

Theorem 2 guarantees the exponential convergence of agents to the desired trajectory after the resolution of all conflicts. Yet, similar to other potential field-based methods, deadlocks can still occur if a conflict persists. The following section addresses this issue.

3.3 Deadlocks. A common drawback of potential field methods is the occurrence of deadlocks, that is, when a vehicle cannot reach its desired destination due to persistent interaction with other agents. These situations are due to symmetries between the tracking and avoidance control, i.e., when $\mathbf{u}_i^a \to -\ddot{\mathbf{z}}_i^d - K_v(\dot{\mathbf{z}}_i^d - \dot{\mathbf{z}}_i) - K_p(\mathbf{z}_i^d - \mathbf{z}_i)$. For damped systems with constant desired trajectories, this condition reduces to $\mathbf{u}_i^a \to -K_p(\mathbf{z}_i^d - \mathbf{z}_i)$ [29]. To break the symmetry and aid in conflict resolution, we propose adding the perpendicular perturbation (11c). Note that $\mathbf{u}_i^p \approx \mathbf{0}$ when the vehicle is still in motion (particularly for large λ_2) and is only active when the avoidance control is active (i.e., under the presence of a collision threat). In Ref. [9], it is shown that these perpendicular perturbations can aid in conflict resolution. Finally, it is worth mentioning that different from Refs. [9,29], the perturbation control proposed in (11c) is almost everywhere continuous and smooth.

Even with this control perturbation, we cannot guarantee that the vehicles will always converge to $\mathbf{z}_i^d$, particularly under the presence of static obstacles. For instance, vehicles may be trapped between large obstacles, walls, or dead-end corridors, which is a common drawback of all previous approaches [9]. In decentralized scenarios where agents have limited information about their surroundings, such as the problem presented herein, the vehicles may need to apply other heuristic measures (e.g., exploration).

4 Numerical Example

In this section, we present an example with vehicles and obstacles of rectangular shape.

4.1 Minimum Safe Distance. Assume the shapes of the ith and jth vehicles can be approximated by rectangles with length ℓ_i, ℓ_j and width w_i, w_j. Without loss of generality, let their lengths be aligned with the x-axis (as shown in Fig. 1). Define the following orientation-dependent functions:

$$\beta_{ij} = \frac{\ell_i}{2} + \frac{\ell_j}{2}\sqrt{\varepsilon^2 + \cos^2\tilde{\phi}_{ij}} + \frac{w_j}{2}\sqrt{\varepsilon^2 + \sin^2\tilde{\phi}_{ij}} \tag{21a}$$

$$\gamma_{ij} = \frac{w_i}{2} + \frac{\ell_j}{2}\sqrt{\varepsilon^2 + \sin^2\tilde{\phi}_{ij}} + \frac{w_j}{2}\sqrt{\varepsilon^2 + \cos^2\tilde{\phi}_{ij}} \tag{21b}$$

where $\varepsilon > 0$ is a small constant chosen for smoothness and $\tilde{\phi}_{ij} = \phi_i - \phi_j$ is the relative orientation. Let $\theta_{ij} = \text{atan2}(z_{j,2} - z_{i,2}, z_{j,1} - z_{i,1})$ represent the angle between $\mathbf{z}_i$ and $\mathbf{z}_j$. Then, the equation for a rectangle with sides β_{ij} and γ_{ij} in polar coordinates ρ_{ij} and θ_{ij}, rotated by ϕ_i and centered at $\mathbf{z}_i$, can be approximated by

$$\zeta_{ij} = \sqrt{\varepsilon^2 + (\gamma_{ij}\cos(\theta_{ij} - \phi_i) + \beta_{ij}\sin(\theta_{ij} - \phi_i))^2} \tag{22a}$$

$$\eta_{ij} = \sqrt{\varepsilon^2 + (\gamma_{ij}\cos(\theta_{ij} - \phi_i) - \beta_{ij}\sin(\theta_{ij} - \phi_i))^2} \tag{22b}$$

$$\rho_{ij} = \frac{2\beta_{ij}\gamma_{ij}}{\zeta_{ij} + \eta_{ij} - 2\varepsilon} \tag{22c}$$

Following the same procedure for the jth agent and using the continuous differentiable approximation of the minimum function [30], one can obtain a smooth function for r_{ij}

$$r_{ij} = r_{ji} = \delta\sqrt{\frac{2}{\rho_{ij}^{-\delta} + \rho_{ji}^{-\delta}}} \tag{23}$$

where $\delta \ge 2$. Choosing smaller $\varepsilon \to 0$ and larger $\delta \to \infty$ yields more compact envelopes. Figure 2 illustrates r_{ij} for different relative orientations between two vehicles of different sizes. The solid line represents the minimum safe distance that the center of the jth agent can come from the ith vehicle, which is generally shorter than the constant minimum distance scenario.

4.2 Simulations. We consider a scenario of $N = 4$ identical vehicles with nonlinear dynamics given by (1). The vehicles are assumed to have rectangular shapes with physical and control

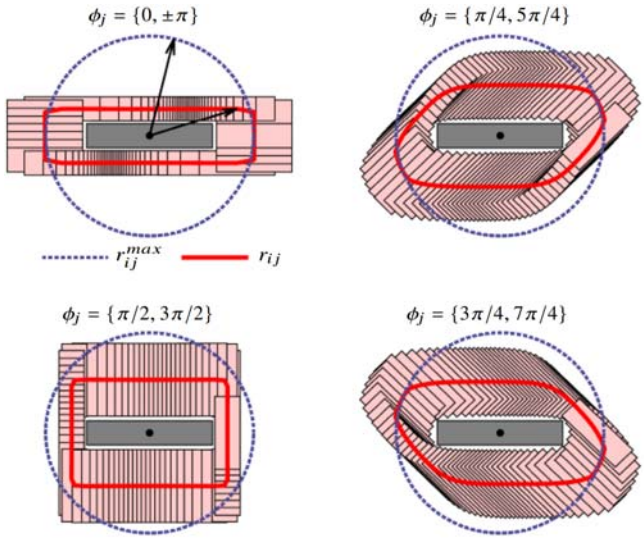

Fig. 2 Comparison between the proposed minimum safe distance framework (solid line) and the conservative use of a constant radius r_{ij}^{max} (in dashed line) for different relative orientations. The ith vehicle is represented by the gray rectangles. The jth vehicle is illustrated in different relative positions and orientations by the light rectangular shapes. The vehicles have dimensions $\ell_i = 5w_i$, $\ell_j = 3w_j$, and $w_i = w_j$.

parameters given as: $m_i = 1\,\text{kg}$, $J_i = 1\,\text{kg}\cdot\text{m}^2$, $\ell_i = 2\,\text{m}$, $w_i = 1\,\text{m}$, $L_i = 2/3\,\text{m}$, $R = 6\,\text{m}$, $K_p = 0.5\,\text{N/m}$, $K_v = 1\,\text{N}\cdot\text{s/m}$, $\lambda_1 = 5$, $\lambda_2 = 3$, and $\lambda_3 = 1$. The vehicles are tasked with following trajectories $\mathbf{z}_i^d(t) = [z_{i,1}^d(t),\, z_{i,2}^d(t)]^T$ defined as

$$z_{i,1}^d(t) = 0.9(t-20) \quad \forall\, i \in \{1,2,3,4\} \tag{24a}$$

$$z_{1,2}^d(t) = -z_{2,2}^d(t) = -\frac{\left(z_{2,1}^d\right)^3}{9^3}, \quad z_{3,2}^d(t) = -z_{4,2}^d(t) = -\frac{\left(z_{4,1}^d\right)^3}{12^3} \tag{24b}$$

which all pass through a single small static obstacle and between two large static obstacles (or walls) whose shapes are approximated by an arrangement of $2\times 2\,\text{m}^2$ squares. Figure 3(top) illustrates the desired trajectories, the vehicles' initial configurations, and the location of static obstacles.

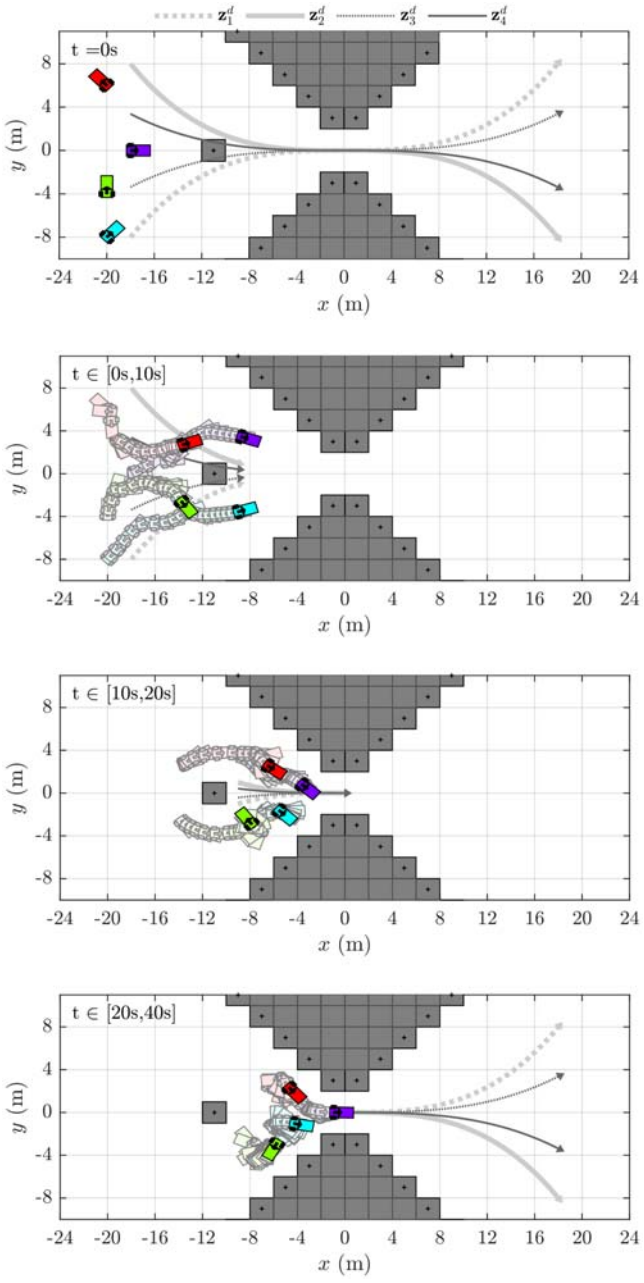

Fig. 3 Sequential motion of vehicles with constant minimum safe distance $r_{ij}^{\max}$. The top figure illustrates the initial configurations and desired trajectories. Other figures illustrate the sequential motion plotted every 0.5 s. Obstacles are represented by gray squares.

We first simulate the system assuming the conventional potential field-based approach of a constant minimum safe distance. Since the circumradius for the vehicles and the obstacles is $\sqrt{1.25}\,\text{m}$ and $\sqrt{2}\,\text{m}$, respectively, we choose $r_{ij} = r_{ij}^{\max} = 2.24\,\text{m}$ as the minimum safe distance with other vehicles and $r_{ij} = r_{ij}^{\max} = 2.53\,\text{m}$ with obstacles. We also choose $\Delta_R = 2\,\text{m}$, for a constant reaction distance of $R_{ij} \in \{4.24\,\text{m}, 4.53\,\text{m}\}$. The system's response can be seen in Fig. 3, where all agents navigate safely but cannot reach the other side of the domain despite the walls having a separation of 4 m. Figure 4 illustrates the position errors, which keep increasing over time.

The response of the multi-vehicle system with the proposed control strategy is illustrated in Fig. 5, where we approximated the rectangular shapes using (22) and (23), for $\varepsilon = 0.01$ and $\delta = 6$. Observe that all vehicles are able to track the desired trajectory and transit through a narrow passage safely. In addition, Fig. 6 shows that the agents eventually converge to the desired trajectory once collision threats are over. Finally, the control input force and

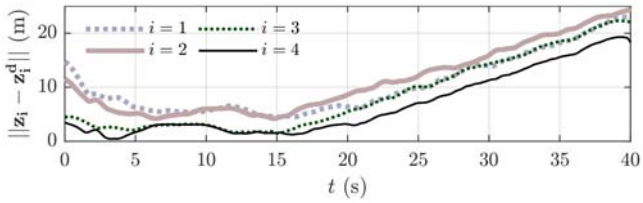

Fig. 4 Position errors when using a constant minimum safe distance

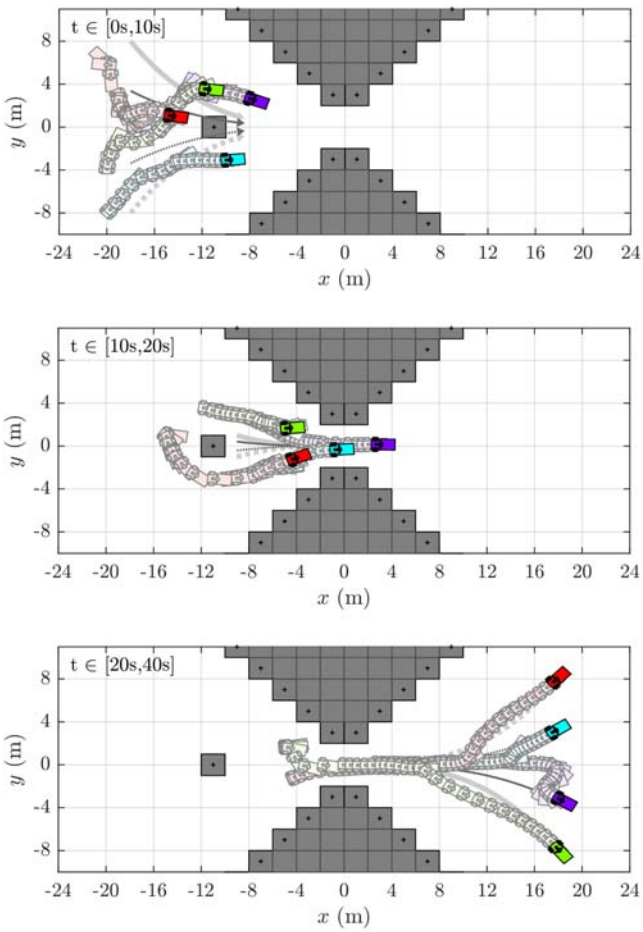

Fig. 5 Sequential motion of vehicles with proposed time-varying orientation-based minimum safe distance r_{ij}

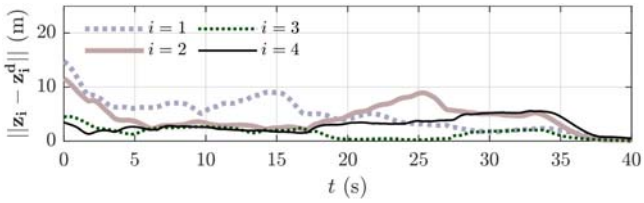

Fig. 6 Position errors when using proposed time-varying orientation-based minimum safe distance

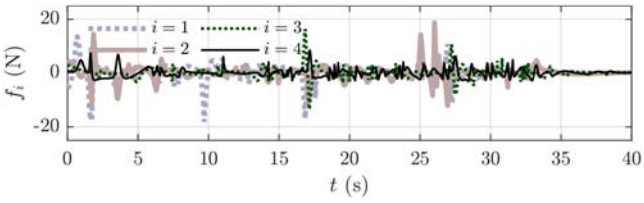

Fig. 7 Control input force when using proposed time-varying orientation-based minimum safe distance

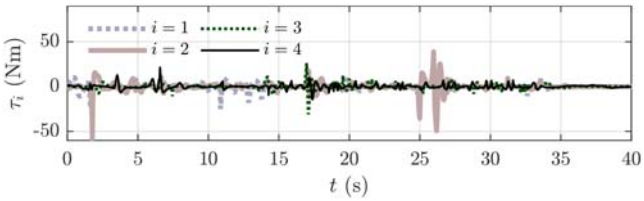

Fig. 8 Control input torque when using proposed time-varying orientation-based minimum safe distance

torque are given in Figs. 7 and 8, respectively, where it can be observed that the control inputs are bounded and continuous.

5 Conclusions

This letter presents a decentralized, reactive collision avoidance framework for nonholonomic systems of unicycle type and arbitrary shape. The framework is built upon the concept of avoidance functions but exploits the use of a novel non-constant minimum safe distance radius that explicitly considers the shape of vehicles and obstacles, as well as their relative position and orientation. In contrast to previous potential field-based methods, the proposed framework only requires a single function between pairs of agents and generates analytical, smooth control inputs. The overall control strategy is rigorously proven to avoid collisions at all times and to converge exponentially to the desired trajectory once all conflicts have been resolved. To the authors' knowledge, this is the first provably safe approach to use a time-varying avoidance radius or minimum safe distance within the avoidance functions framework.

Conflict of Interest

There are no conflicts of interest.

Data Availability Statement

The datasets generated and supporting the findings of this article are obtainable from the corresponding author upon reasonable request.

References

[1] Fiorini, P., and Shiller, Z., 1998, "Motion Planning in Dynamic Environments Using Velocity Obstacles," Int. J. Rob. Res., **17**(7), pp. 760–772.

[2] van den Berg, J., Snape, J., Guy, S. J., and Manocha, D., 2011, "Reciprocal Collision Avoidance With Acceleration-Velocity Obstacles," IEEE International Conference on Robotics and Automation, Shanghai, China, May 9–13, pp. 3475–3482.

[3] Guo, K., Wang, D., Fan, T., and Pan, J., 2021, "VR-ORCA: Variable Responsibility Optimal Reciprocal Collision Avoidance," IEEE Rob. Autom. Lett., **6**(3), pp. 4520–4527.

[4] Chakravarthy, A., and Ghose, D., 1998, "Obstacle Avoidance in a Dynamic Environment: A Collision Cone Approach," IEEE Trans. Syst. Man Cybern. A Syst. Humans, **28**(5), pp. 562–574.

[5] Haraldsen, A., Wiig, M. S., and Pettersen, K. Y., 2023, "Dynamic Obstacle Avoidance for Nonholonomic Vehicles Using Collision Cones: Theory and Experiments," Proceedings of IEEE Conference on Control Technology and Applications, Bridgetown, Barbados, Aug. 16–18, pp. 46–52.

[6] Khatib, O., 1986, "Real-Time Obstacle Avoidance for Manipulators and Mobile Robots," Int. J. Rob. Res., **5**(1), pp. 90–98.

[7] Stipanović, D. M., Hokayem, P. F., Spong, M. W., and Šiljak, D., 2007, "Cooperative Avoidance Control for Multiagent Systems," ASME J. Dyn. Syst. Meas. Control, **129**(5), pp. 699–707.

[8] Mastellone, S., Stipanović, D. M., Graunke, C. R., Intlekofer, K. A., and Spong, M. W., 2008, "Formation Control and Collision Avoidance for Multi-agent Non-holonomic Systems: Theory and Experiments," Int. J. Rob. Res., **27**(1), pp. 107–126.

[9] Zhang, W., Rodríguez-Seda, E. J., Deka, S., Amrouche, M., Zhou, D., Stipanovic, D., and Leitmann, G., 2029, "Avoidance Control With Relative Velocity Information for Lagrangian Dynamics," J. Intell. Rob. Syst., **99**, pp. 229–244.

[10] Glotfelter, P., Cortés, J., and Egerstedt, M., 2017, "Nonsmooth Barrier Functions With Applications to Multi-robot Systems," IEEE Contr. Syst. Lett., **1**(2), pp. 310–315.

[11] Chen, Y., Singletary, A., and Ames, A. D., 2021, "Guaranteed Obstacle Avoidance for Multi-Robot Operations With Limited Actuation: A Control Barrier Function Approach," IEEE Control Syst. Lett., **5**(1), pp. 127–132.

[12] Rodríguez-Seda, E. J., Tang, C., Spong, M. W., and Stipanović, D. M., 2014, "Trajectory Tracking With Collision Avoidance for Nonholonomic Vehicles With Acceleration Constraints and Limited Sensing," Int. J. Rob. Res., **33**(12), pp. 1569–1592.

[13] Huang, S., Teo, R. S. H., and Tan, K. K., 2019, "Collision Avoidance of Multi Unmanned Aerial Vehicles: A Review," Annu. Rev. Control, **48**, pp. 147–164.

[14] Tang, J., Lao, S., and Wan, Y., 2022, "Systematic Review of Collision-Avoidance Approaches for Unmanned Aerial Vehicles," IEEE Syst. J., **16**(3), pp. 4356–4367.

[15] Sunkara, V., Chakravarthy, A., and Ghose, D., 2019, "Collision Avoidance of Arbitrarily Shaped Deforming Objects Using Collision Cones," IEEE Rob. Autom. Lett., **4**(2), pp. 2156–2163.

[16] Minguez, J., and Montano, L., 2009, "Extending Collision Avoidance Methods to Consider the Vehicle Shape, Kinematics, and Dynamics of a Mobile Robot," IEEE Trans. Rob., **25**(2), pp. 367–381.

[17] Borenstein, J., 1994, "Real-Time Obstacle Avoidance for Non-point Mobile Robots," Proceedings of World Conference on Robotics Research, Pittsburgh, PA, Sept. 17–19, 1991.

[18] Wu, Z., Hu, G., Feng, L., Wu, J., and Liu, S., 2016, "Collision Avoidance for Mobile Robots Based on Artificial Potential Field and Obstacle Envelope Modelling," Assembly Autom., **36**(3), pp. 318–332.

[19] Braquet, M., and Bakolas, E., 2022, "Vector Field-Based Collision Avoidance for Moving Obstacles With Time-Varying Elliptical Shape," Proceedings of Modeling, Estimation, and Control Conference, Jersey City, NJ, Oct. 2–5, pp. 587–592.

[20] Xie, H., Patel, R., Kalaycioglu, S., and Asmer, H., 1998, "Real-Time Collision Avoidance for a Redundant Manipulator in an Unstructured Environment," Proceedings of IEEE/RSJ International Conference on Intelligent Robots and Systems, Victoria, BC, Canada, Oct. 17, Vol. 3, pp. 1925–1930.

[21] Zimmermann, S., Busenhart, M., Huber, S., Poranne, R., and Coros, S., 2022, "Differentiable Collision Avoidance Using Collision Primitives," IEEE/RSJ International Conference on Intelligent Robots and Systems, Kyoto, Japan, Oct. 23–27, p. 8086–8093.

[22] Zhang, X., Liniger, A., and Borrelli, F., 2021, "Optimization-Based Collision Avoidance," IEEE Trans. Control Syst. Technol., **29**(3), pp. 972–983.

[23] Hu, Y., Fu, J., and Wen, G., 2023, "Decentralized Robust Collision-Avoidance for Cooperative Multirobot Systems: A Gaussian Process-Based Control Barrier Function Approach," IEEE Trans. Control Network Syst., **10**(2), pp. 706–717.

[24] Brockett, R. W., 1983, "Asymptotic Stability and Feedback Stabilization," *Differential Geometric Control Theory*, R. W. Brockett, R. S. Millman, and H. J. Sussmann, eds., Birkhauser, Boston, MA, pp. 181–191.

[25] Sarkar, N., Yun, X., and Kumar, V., 1994, "Control of Mechanical Systems With Rolling Constraints: Application to Dynamic Control of Mobile Robots," Int. J. Rob. Res., **13**(1), pp. 55–69.

[26] Rodríguez-Seda, E. J., and Stipanović, D. M., 2020, "Cooperative Avoidance Control With Velocity-Based Detection Regions," IEEE Control Syst. Lett., **4**(2), pp. 432–437.

[27] Rodríguez-Seda, E. J., 2024, "Decentralized Low-Energy Avoidance Control Framework for Multiple Mobile Agents Using Irregular Observations," IEEE Trans. Control Syst. Technol., **32**(5), pp. 1027–1039.

[28] Khalil, H. K., 2002, *Nonlinear Systems*, Prentice Hall, Upper Saddle River, NJ.

[29] Rodríguez-Seda, E. J., and Stipanović, D. M., 2013, "Guaranteed Collision Avoidance With Discrete Observations and Limited Actuation," Advances in Intelligent Vehicles, Y. Chen, and L. Li, eds., Intelligent Systems, Academic Press, Boston, MA, pp. 89–110.

[30] Stipanović, D. M., Tomlin, C. J., and Leitmann, G., 2012, "Monotone Approximations of Minimum and Maximum Functions and Multi-Objective Problems," Appl. Math. Optim., **66**(3), pp. 455–473.